Guidelines for observing time estimates with the NIKA2 continuum camera at the IRAM-30m Telescope

Sommer Semester 2017

P. García, F.-X. Désert, S. Leclercq, C. Kramer, & A. Sievers

January 29, 2017

Abstract

The present document explains how the total integration time t_{total} for a given map size to be observed with the NIKA2 camera is calculated. The formula for t_{total} is derived step-by-step and the python script used to calculate t_{total} is described using two examples, for point-like and extended sources. In Appendix A, the prediction accuracy of t_{total} is tested against simulated observations of the On-The-Fly (OTF) mapping mode with NIKA2, showing an agreement within 40% (worst case) wrt. the average integration time within the observed area. The python script used to calculate t_{total} is described using two examples, for point-like and extended sources. This manuscripts is partially based on the previous document for GISMO and NIKA observations [1], calculations done by F.-X. Désert, and simulations of the NIKA2 On-The-Fly (OTF) observing mode by P. García.

1 The NIKA2 Camera

The *New IRAM KID Array 2* (NIKA2) camera is the kilo-pixel expansion of the NIKA prototype camera. It is a dual-band imaging camera built for the 30m telescope [2, 3, 4] by an international consortium lead by Alain Benoit and Alessandro Monfardini from the *Institut Néel* in Grenoble, France. The camera is equipped with a novel type of superconducting detectors called KIDs (Kinetic Inductance Detectors). The focal plane consists of three filled arrays: a 2 mm array, and two 1.2 mm arrays for horizontal and vertical polarization measurements. They operate at 100 mK, delivered by a continuous closed-cycle dilution fridge, and optimized for observations in the atmospheric windows at 2 mm and 1.2 mm. A dichroic is used to split the long/short wavelengths such that both channels observe the sky simultaneously with a common instantaneous field-of-view (FoV) of 6.5' in diameter. The 2 mm (1.2 mm) array is made up of 616[1] (2×1140 for Horizontal and Vertical polarizations) square pixels. Currently, the observing mode for **extended and point sources** with NIKA2 is the OTF observing mode, in which while the telescopes drives continuously in a certain direction, data and positional information are recorded for later map reconstruction (See Appendix A for a schematic view of the OTF scanning pattern). More information about NIKA2 can be found at the dedicated `IRAM web site`.

2 Observing Time Estimate

The expected noise flux density per beam of a map is given by:

$$\sigma = \frac{\mathrm{NEFD}}{\sqrt{t_{beam}}}, \tag{1}$$

[1] This number corresponds to the array installed in Sept. 2016.

where σ is expressed in [mJy/beam], NEFD is the Noise Equivalent Flux Density in [mJy$\cdot\sqrt{s}$], and t_{beam} is the integration time per beam in seconds. The NEFD can further be expressed as:

$$\mathrm{NEFD} = \mathrm{NEFD}_0 \cdot e^{\tau/\sin(el)} \cdot h_{filter}, \tag{2}$$

where NEFD_0 is the instrumental NEFD without the atmosphere, τ is the zenith opacity at the reference frequency, *el* is the source elevation in radian, and h_{filter} is a dimensionless factor that accounts for post-processing noise filtering. The sensitivity penalty for retrieving extended emission in NIKA2 observations leads to values $1.0 \leqslant h_{filter} \leqslant 2.0$, depending on the source extent.

The **integration time per beam** is derived from the total integration time of the observation t_{int} (excluding overheads), the FoV of the camera, and the area covered by the observations. If the scanning pattern covers a rectangular area A_{map} of sides Δ_x and Δ_y, then the integration time per beam is expressed as:

$$t_{beam} = \frac{A_{FoV}}{A_{map}} \cdot t_{int}, \tag{3}$$

where $A_{map} \sim \Delta_x \cdot \Delta_y + A_{FoV}$, and the ratio A_{FoV}/A_{map} represents the average fractional coverage[2] of the map. Notice that the $\Delta_x \cdot \Delta_y$ area is the area covered by the central pixel of the array, as shown in the upper right panel of Figure 1. Due to differences in performance, a small fraction of the pixels covering the camera FoV will not be available for the measurements (bad pixels), reducing the nominal FoV area to an *effective* FoV area. If the fraction of good pixels in the array is f_{pix}, then the effective FoV area of the camera can be expressed as $f_{pix} \cdot A_{FoV}$.

Putting the above information together, the following general formula that describes the total observing time t_{total} required to reach a given flux uncertainty of σ is obtained:

$$\boxed{t_{total} = \left(\frac{\mathrm{NEFD}_0 \cdot e^{\tau/\sin(el)}}{\sigma} \cdot h_{filter}\right)^2 \times \left(1 + \frac{\Delta_x \cdot \Delta_y}{f_{pix} A_{FoV}}\right) \times h_{overhead}} \tag{4}$$

The $h_{overhead}$ factor accounts for telescope overheads (slewing, pointing, focusing, calibration), i.e. all telescope time which is not spend integrating on-source. This overhead factor depends strongly on the observing project. For instance, deep integrations on a single source lead to small overheads while short integrations on multiple sources spread over the sky lead to significantly larger overheads due to the increased telescope slew time. We recommend to use $1.5 \leqslant h_{overhead} \leqslant 2.0$, depending on the project. The right term within brackets accounts for small maps where a point source is always within the FoV (so there is always time ON-source in the OTF scans), and larger maps, where the FoV goes OFF-source a fraction of the time. In order to achieve an homogeneous RMS distribution within the $\Delta_x \cdot \Delta_y$ area, we recommend to carry out maps with lengths $\geqslant 2$ [arcmin]. In Equation 4, is it assumed that for 1.2 mm observations, both horizontal and vertical polarizations are combined for the estimation of t_{total}. Table 1 summarizes the NIKA2 instrument's specifications while in Table 2 the parameters used in the time estimator are listed. For deep integrations ($< 0.5 - 1$ [mJy/beam]) we remind proposers to consider estimating confusion noise levels as it might prevent reaching such low rms values. Also useful for large scale mapping is to estimate the mapping speed of the array in units of [arcmin^2 hour^{-1} mJy^{-2}]. This can be derived by noticing that the total integration time in Equation 4 can be expressed as:

$$t_{total} = \left(\frac{A_{map}}{S_{map}}\right) \times \frac{1}{\sigma^2}, \tag{5}$$

where S_{map} is the mapping speed of the array. Using Equations 2 and 4, solving for S_{map} we obtain:

[2]Note that the approximation $A_{map} \sim \Delta_x \cdot \Delta_y + A_{FoV}$ overestimates the covered area if the source stays on-array during the observation, in which case $t_{beam} \sim t_{int}$. For a detailed derivation of this approximation see Appendix A

$$S_{map} = \left(\frac{\Delta_x \cdot \Delta_y}{NEFD^2} \right) \times \frac{1}{h_{overhead}}. \quad (6)$$

The values of the mapping speed for the example cases in Section 3 are listed in Table 3. In Appendix A, the predictions from Equation 4 are compared with simulations of the NIKA2 OTF observing mode.

Table 1: NIKA2 instrument's specifications [5].

Definition	Symbol	NIKA2	
Band		1	2
Central Wavelength	λ [mm]	1.2	2.0
Central Frequency	ν [GHz]	260	150
Frequency Bandwidth	$\Delta\nu$ [GHz]	240 – 280	125 – 170
Number of pixels	N_{pix}	2×1140	616
Pixel Spacing	[Fλ]	0.9	
Half-Power Beam Width (HPBW)	Θ_{res} [arcsec]	12	18

Table 2: Parameters used in the time estimator.

Definition	Symbol	NIKA2	
Band		1	2
Noise equivalent flux density	$NEFD_\circ$ [mJy·$\sqrt{s}$]	30[1]	15
Field-of-View diameter	D_{FoV} [arcmin]	6.5	
Field-of-View area	A_{FoV} [arcmin^2]	33.2	
Fraction of good pixels	f_{pix}	0.75	
Post-processing overhead	h_{filter}	$1.0 \lesssim h_{filter} \lesssim 2.0$	
Telescope overheads	$h_{overhead}$	$1.5 \lesssim h_{overhead} \lesssim 2.0$	
Noise goal	σ [mJy]	user defined	
x-length of A_{map}	Δ_x [arcmin]	user defined	
y-length of A_{map}	Δ_y [arcmin]	user defined	

[1] The sensitivity at 1.2 mm is obtained after combining the measurements of the two 1.2 mm arrays. No polarization measurement is provided for the time being.

3 Time Estimator Test Cases

A *python* script performs the calculations to obtain the total integration time for a given project. A help menu describing each script's option is displayed by running the following instruction in a terminal:

```
> python NIKA2_Time_Estimator.py --help
```

In the following, some illustrative examples of the time estimator results for OTF mapping are presented. These are summarized in Table 3 and typical weather conditions at the 30m telescope's site are compiled in Table 4.

- **Point Source:** to observe a single point source of flux 1 [mJy/beam] at 2 mm and 1.5 [mJy/beam] at 1.2 mm with NIKA2, we would use the OTF observing mode with $\Delta_x = \Delta_y = 2'$, and the most aggressive filtering scheme for with $h_{filter} = 1.0$, which is optimized for point source photometry. For a 5-σ detection of this source, one requires a flux uncertainty $\sigma = 0.2$ [mJy/beam] at 2 mm and at 0.3 [mJy/beam] at 1.2 mm. Assuming 4 mm of precipitable water vapor (pwv), i.e. an opacity $\tau \sim 0.10$ at 2 mm and $\tau \sim 0.30$ at 1.2 mm, and a typical source elevation of 50 degrees, Equation 4 gives a total observing time of 3.5 hours for the 2.0 mm band, and 10.6 hours for the 1.2 mm band, including overheads ($h_{overhead} \sim 1.5$). Note that in practice we would split this long observation into smaller observing blocks.

- **Nearby Galaxy:** to observe a nearby galaxy of size $\Delta_x = \Delta_y = 15'$, where extended emission at a level of 2.22 [mJy/beam] at 1.2 mm and 1.26 [mJy/beam] at 2 mm shall be detected, we would use the OTF observing mode with the least aggressive filtering scheme with $h_{filter} = 2.0$, which is optimized for extended emission. For a 3-σ detection of this source, one requires a flux uncertainty $\sigma = 0.74$ [mJy/beam] and 0.42 [mJy/beam] for the 1.2 mm and 2 mm bands, respectively. Assuming 2 mm of precipitable water vapor (pwv), i.e. an opacity $\tau \sim 0.15$ at 1.2 mm and $\tau \sim 0.05$ at 2 mm, and a typical source elevation of 45 degrees, Equation 4 gives a total observing time of 32.9 hours for the 2.0 mm band and an observing time of 56.2 hours for the 1.2 mm band, including overheads ($h_{overhead} \sim 2.0$). Note that in practice we would split this long observation into smaller observing blocks.

Table 3: Summary of time estimates in Section 3 and average pwv values in Summer/Winter conditions

source	**Point Source**		**Nearby Galaxy**	
band	1.2 mm	2.0 mm	1.2 mm	2.0 mm
Δ_x [arcmin]	2	2	15	15
Δ_y [arcmin]	2	2	15	15
pwv [mm]	4	4	2	2
τ	0.30	0.10	0.15	0.05
El [deg]	50	50	45	45
h_{filter}	1.0	1.0	2.0	2.0
$h_{overhead}$	1.5	1.5	2.0	2.0
rms [mJy/beam]	0.30	0.20	0.74	0.42
	Total Integration Time Results			
$\mathbf{t}_{spec}$ [hours]	10.6	3.5	56.2	32.9
	Mapping Speed			
$\mathbf{S}_{map}$ [arcmin^2 hour^{-1} mJy^{-2}]	4.9	32.8	73.4	389.6

Table 4: Typical Summer/Winter weather conditions at the 30m telescope's site

	Winter Conditions			**Summer Conditions**		
	excellent	**good**	**average**	**excellent**	**good**	**average**
pwv [mm]	1	2	4	2	4	7
τ (1.2 mm band)	0.08	0.15	0.30	0.15	0.30	0.53
τ (2.0 mm band)	0.03	0.05	0.10	0.05	0.10	0.18

A Comparison of the Total Integration Time with Simulations

In the following, the results of our NIKA2 OTF simulations are compared with the prediction for the total integration time in Equation 4. We also check the accuracy of the map area approximation used to obtain the same equation.

A.1 Description of the Simulations

To test the prediction capabilities of Equation 4 to estimate the total integration time required for given observations requirements, we have performed simulations of the NIKA2 OTF scan pattern for the goal ($f_{pix} = 0.9$) and specification ($f_{pix} = 0.6$) values of the fraction of good pixels in the NIKA2 arrays. In the simulations we have assumed a beam size of 11", a space sampling of 11" in both scan directions, and an integration time per resolution element of 1 [s].

In Figure 1, the simulation results of the NIKA2 OTF observing mode for $\Delta_x = \Delta_y = 15$ [arcmin] and for $f_{pix} = 0.6$, are shown. A schematic view of the OTF scanning strategy is shown in upper left panel of the figure. A fake astronomical source is shown in color scale together with its astronomical coordinates depicted as a white cross at (0,0) offsets. The field-of-view (FoV) covered by the NIKA2 camera (solid black circle) and its resolution elements or pixels (small circles within FoV) are also shown. The fraction of good pixels (filled circles) within the FoV is 0.60 in the example, while the map size (Δ_x and Δ_y values) and OTF line spacing (Step) is given at the top of the plot. The path of the central pixel of the array while scanning each OTF line within the $\Delta_x \cdot \Delta_y$ area is shown as solid straight lines while the scanning directions are also displayed. The total area covered by the array while performing the OTF scans is enclosed in the dotted line. Such an OTF scan will produce an integration time spatial distribution as shown in the upper-right panel of the same figure, represented by the color scale, and where it is assumed that the integration time per dump is 1 s. The solid line black circle corresponds to the FoV area (A_{FoV}) and the map size is shown as a square with dashed-lines. The spatial sampling of the simulated observations is given by the Stepx and Stepy variables at the top of the figure, which in this case corresponds to the assumed beam size (11") in both scan directions. As expected, the integration time per position decreases towards the edges of the map. For a typical elevation of 45°, good weather conditions with opacity $\tau = 0.1$, and a Noise Equivalent Flux Density without the atmosphere ($NEFD_0$) of 30 [mJy$\cdot\sqrt{s}$], the integration time is converted into the spatial RMS noise distribution shown in the bottom-left panel of Figure 1. This distribution is smoother than the integration time spatial distribution as expected, since the RMS noise scales as the inverse square-root of the integration time $\sigma \propto 1/\sqrt{t}$. From the RMS noise spatial distribution, an histogram is calculated. In order to find the best characterization of the OTF map in terms of its RMS noise, several RMS noise estimates are overplotted on the histogram in Figure 1 as vertical solid lines. From the histogram itself, the RMS noise of the histogram's peak (blue), the center of a Gaussian fit to the histogram (black), and the counts-weighted average of the RMS noise axis (green) are plotted. From within the $\Delta_x \cdot \Delta_y$ area, the minimum (yellow), average (red), and maximum (orange) RMS noise derived from the maximum, average, and minimum time per position are also plotted.

A.2 Effective Area Approximation

The approximation $A_{map} \sim \Delta_x \cdot \Delta_y + A_{FoV}$ is used in deriving Equation 4. We checked the accuracy of such approximation against our definition of the *effective area* of a given OTF map. The total area covered by the array (dotted line in the upper left panel of Figure 1) is given by:

$$A_{total} = \Delta_x \cdot \Delta_y + D_{FoV}(\Delta_x + \Delta_y) + A_{FoV}, \tag{7}$$

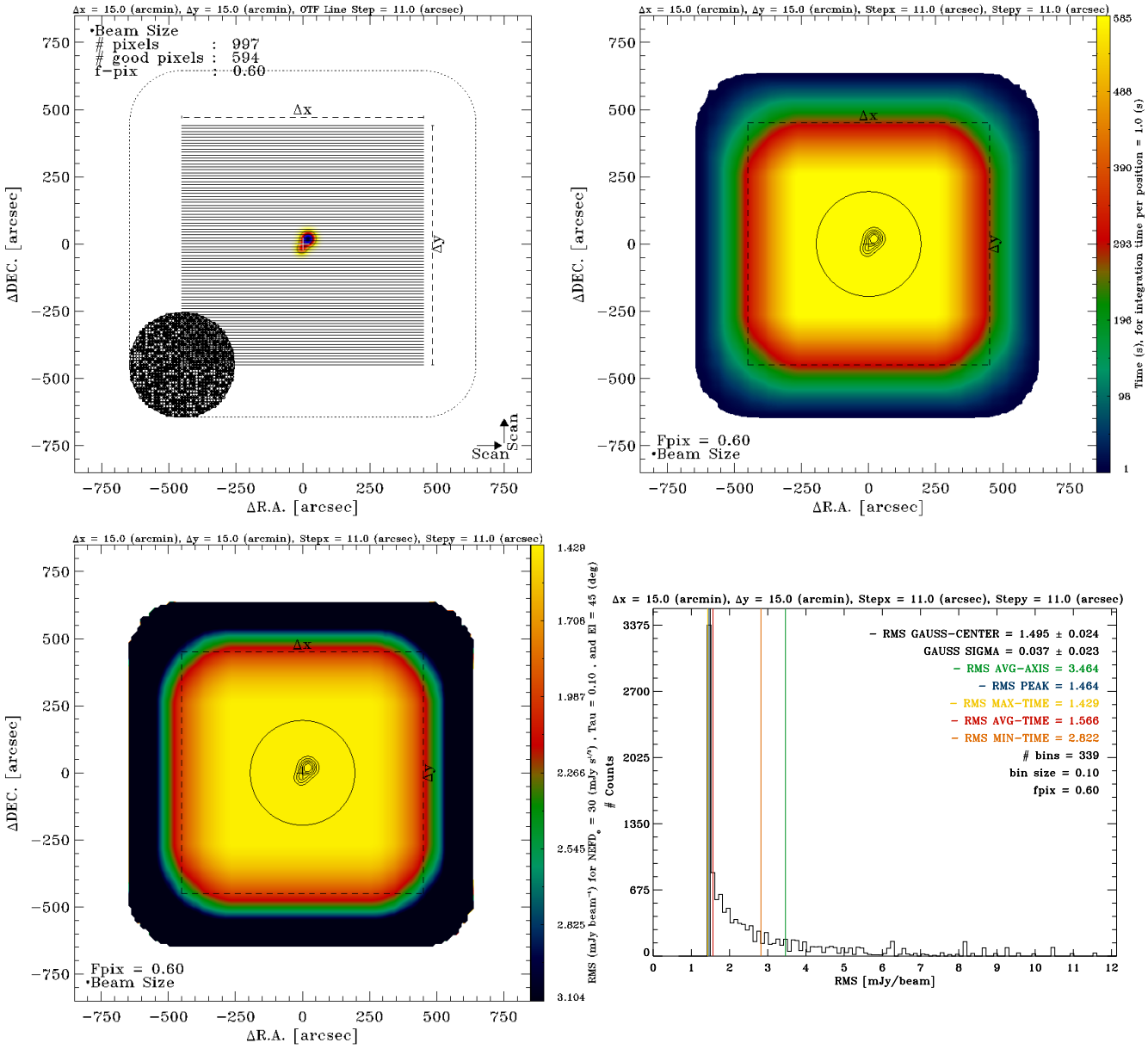

Figure 1: **Top-left**: Schematic view of an OTF map of size $\Delta x \cdot \Delta y$ with NIKA2. The individual resolution elements (small filled/empty circles) within the FoV are also shown. The assumed beam size is 11". The path of the central pixel during the OTF scans is represented as solid lines. The total area covered by the array is enclosed by the dotted line. **Top-right**: Integration time spatial distribution produced by the OTF scan strategy in the top-left panel. Larger integration times are found towards the center of the map. The black circle in the center represents the FoV area. The sampling interval in both scanning directions (Stepx and Stepy) is given in the figure. **Bottom-left**: RMS spatial distribution derived from the integration time spatial distribution in the upper right panel. Several RMS values are calculated to characterize the RMS distribution (vertical colored lines). See the main text for an explanation of each derived value.

where $\Delta_x \cdot \Delta_y$ is the area covered by the central pixel of the NIKA2 array, D_{FoV} is the FoV diameter, and A_{FoV} is the FoV area. We define the *effective area* of a given OTF map as:

$$A_{eff} = \sum_i A_{pix} \cdot \sqrt{\frac{t_i}{t_{max}}}, \tag{8}$$

where $A_{pix} = \Theta^2$ is the pixel area (assumed equal for all resolution elements in the array), Θ is the main lobe's FWHM, t_i is the total integration time in the i-th position of the map, and t_{max} is the maximum integration time per position in the observed map. Then, the approximation to A_{eff} is defined as:

$$A_{approx} = \Delta_x \cdot \Delta_y \left(1 + \frac{A_{FoV}}{\Delta_x \cdot \Delta_y}\right). \tag{9}$$

In Figure 2, A_{approx} as a function of A_{eff} for a very large range of map sizes (for $\Delta_x = \Delta_y$, from 1 to 20 [arcmin]) for $f_{pix} = 0.6$ (left panels) and for $f_{pix} = 0.9$ (right panels), is shown. From the figures, it is clear that A_{approx} is in excellent agreement with A_{eff} over the entire map size range. The percentage difference between both quantities is within 8% for map lengths below 10 [arcmin] and reaches a plateau below 12% for large maps where A_{approx} systematically underestimates the effective area. A linear fit to the data points (dotted line, see the formula in the bottom panels) shows a very robust linear correlation, with a slope of 0.87 ± 0.00 for both f_{pix} values.

A.3 Total Integration Time vs. Average Integration Time Within $\Delta_x \cdot \Delta_y$ from the Simulations

In Figure 3 (bottom panels), the total integration time derived from Equation 4 for $f_{pix} = 0.6$ and $f_{pix} = 0.9$ is compared to the average integration time within the area covered by the central pixel $\Delta_x \cdot \Delta_y$. The later values are multiplied by the $(1 + \Delta_x \cdot \Delta_y / f_{pix} A_{FoV})$ factor to take into account the number of resolution elements in the FoV. In order to evaluate the total integration time in Equation 4 we have chosen the peak RMS noise value in the RMS noise histogram derived from the simulated maps (blue vertical line in Figure 1), since it is a good characterization of the expected RMS noise for a given simulated observation. Also, to evaluate the total integration time in Equation 4, $h_{filter} = h_{overhead} = 1$ were assumed. In the figure, filled black circles represent the values from the simulations while gray filled triangles represent the values obtained from Equation 4. The solid lines connecting the points are plotted to identify the general trend with increasing map length.

From the comparison between the simulation results and the predictions from Equation 4, it is clear that the total integration time from the formula closely relates to the average integration time within the $\Delta_x \cdot \Delta_y$ area. For maps slightly larger than the FoV, there is an almost constant difference between simulations and predictions, which is mirrored in the decreasing percentage difference towards larger maps. In this range, the formula is accurate to within 40% (worst case) and improves gradually towards larger maps for both f_{pix} values. For maps smaller than the FoV, the largest percentage differences is greatly reduced to within 15%, but the scatter is larger than for larger maps.

References

[1] Guidelines for observing time estimates with IRAM-30m continuum cameras. N. Billot, C. Kramer, S. Leclercq, I. Hermelo, X. Desert & A. Kovács, August 4, 2014

[2] Improved mm-wave photometry for kinetic inductance detectors. Calvo, M., Roesch, M., Désert, F.-X., et al. 2013, A&A, 551, L12

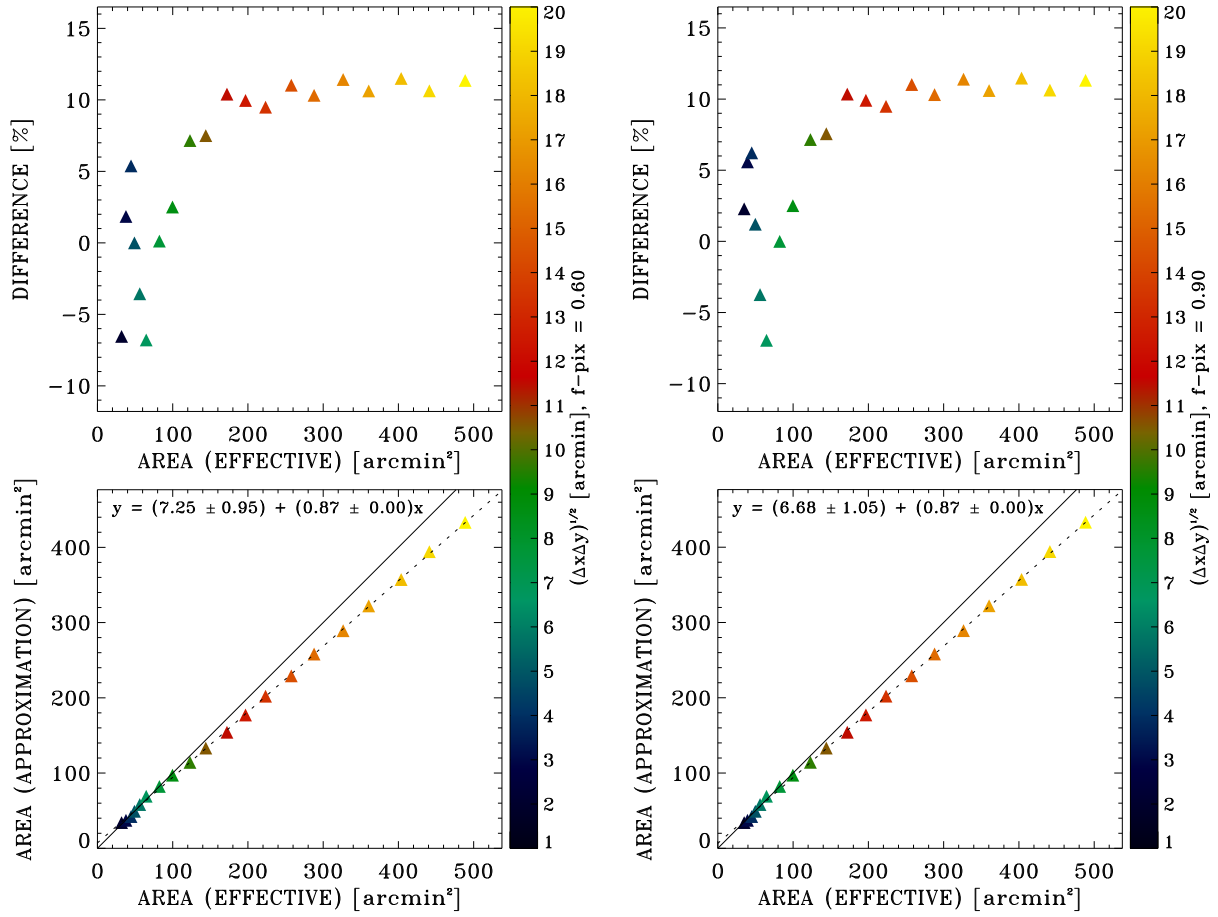

Figure 2: **Bottom**: *effective area* (A_{eff}) as defined in Equation 8 as a function of its approximation (A_{approx}) in Equation 9 over a range of map lengths (for $\Delta_x = \Delta_y$, from 1 to 20 [arcmin]) for $f_{pix} = 0.6$ (left) and for $f_{pix} = 0.9$ (right). A linear fit to the data points is shown within the panels (dotted line). The solid straight line represents the identity. **Top**: percentage difference between A_{eff} and A_{approx}.

[3] Performance and calibration of the NIKA camera at the IRAM 30 m telescope. Catalano, A., Calvo, M., Ponthieu, N., et al. 2014, A&A, 569, A9

[4] The NIKA2 Instrument, A Dual-Band Kilopixel KID Array for Millimetric Astronomy. Calvo, M., Benoit, A., Catalano, A., et al. 2016, arXiv:1601.02774

[5] The NIKA2 commissioning campaign: performance and first results. Catalano, A., Adam, R., Ade, P., et al. 2016, arXiv:1605.08628

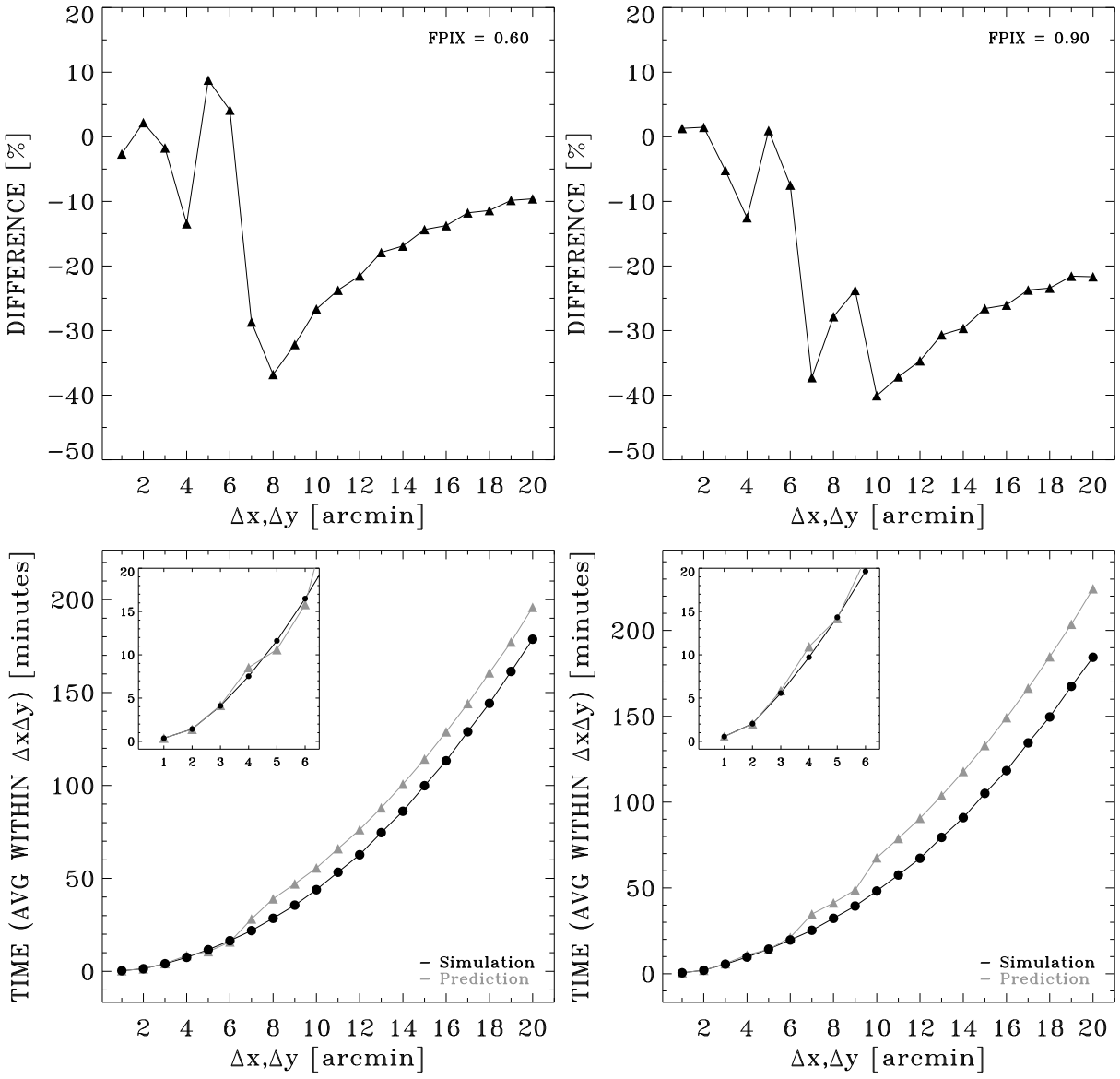

Figure 3: **Bottom panels**: average integration time within the area covered by the central pixel $\Delta_x \cdot \Delta_y$ as a function of map length (in black) for $f_{pix} = 0.6$ (left) and $f_{pix} = 0.9$ (right). The predictions for the total integration time from Equation 4 (in gray) are overplotted. **Upper panels**: percentage difference between both quantities. For both f_{pix} values, the predictions are within 40% of the values obtained from the simulations with large variations depending on map length.